Egyptian Geophysical Society
EGS Journal, Vol. 9, No. 1, 1-11 (2011)

ANALYSIS AND INTERPRETATION OF AIRBORNE GAMMA-RAY SPECTROMETRIC AND AEROMAGNETIC DATA, BIR UM EL FAWAKHIR AREA, CENTRAL EASTERN DESERT, EGYPT

A.A. Khamies
Nuclear Materials Authority, P.O. Box 530, El-Maadi, Cairo, Egypt.

تحليل و تفسير معطيات المسح الجوى الإشعاعى الجامى الطيفى و المغناطيسى فى منطقة بير أم الفواخير وسط الصحراء الشرقية – مصر

الخلاصة: تقع منطقة بير أم الفواخير بين خطى عرض '٥٩ °٢٥ – '٢٣ °٢٦ شمالا وخط طول '١٠ °٣٣ – '٤٠ °٣٣ وتكتسب منطقة الدراسة أهميتها من وجود شواهد مهمة لتواجد اليورانيوم مصاحبا للجرانيت الحديث بها مثل ام حاد، كب عميرى و العرضية كما انها تتضمن العديد من مناجم الذهب القديمة مثل العرضية وعطا الله والفواخير والسد و حمامة. أيضا تتضمن العديد من الحفريات القديمة للذهب عبر نطاق قص متجه شمال غرب– جنوب شرق ممتد لأكثر من ٨٠ كيلو متر من العرضية شمالا الى أم الفواخير جنوبا.

يتناول العمل الحالى تحليل وتفسير بيانات المسح الجامى الطيفى والمغناطيسية الجوية وصور الأقمار الصناعية فى منطقة بير أم الفواخير لشرح العوامل التركيبية المتحكمة فى تواجد التمعدن فى هذه المنطقة. تم مقارنة خرائط العناصر الإشعاعية و نسبها بالخريطة الجيولوجية للمنطقة ومنها تم تحديد النطق عالية المستوى الاشعاعي. اظهرت الخرائط الاشعاعية أن الجزء الجنوبى لكل من كتلتى كب عميرى و أم حاد وكذلك الجزء الشمالى الغربى للعرضية لها محتوى اشعاعى عالي. وفى محاولة لتحليل الشاذات المغناطيسية و ربطها بالتغير الجيولوجى و التراكيب التكتونية تم تطبيق بعض التقنيات المتقدمة تَتضمّنُ هذه التقنياتِ تقنية طيف القدرة، و فصل المجال المغناطيسى للتمييز بين مصادر الشاذات و التباينات الضحلة (المتبقية أو القريبة من السطح) والعميقة (الإقليمية أو الغائرة فى العمق) ، و تقنية المشتقة الرأسية الثانية وتقنية تحليل الاشارة وتقنية حلول أيولر و تقنية تحليل الظلال. وقد لوحظ ان هناك علاقة وثيقة بين المغناطيسية و الملامح الجيولوجية و التركيبية للمنطقة. وقد أدى التكامل بين تطبيق هذه التقنيات إلى رسم خريطة تركيبية لصخور القاعدة المعقدة لتوضيح الإطار الجيولوجى والتركيبى الإقليمى العام لمنطقة الدراسة وتبين من تفسير الخريطة التركيبية وجود مجموعات من الصدوع تأخذ الاتجاه (شمال غرب–جنوب شرق، شمال شرق– جنوب غرب و شمال – جنوب) تتحكم فى الاطار التركيبى للمنطقة كما أنها تشير الى دور النشاط البركانى القاعدى فى السيطرة على مواقع شاذات اليورانيوم و تعدين الذهب على طول نظام صدوع شبه موازية تتجه شمال غرب – جنوب شرق.كما تبين ان هناك تماثلاً بين نظام الصدوع (شمال غرب–جنوب شرق، شمال شرق– جنوب غرب و شمال – جنوب) المستنتجة من الصور الفضائية وتلك التى ظهرت من تحليل الخرائط المغناطيسية

ABSTRACT: *Bir Um El Fawakhir area is located between latitudes 25^0 59'- 26^0 23' N and Longitudes 33^0 10' - 33^0 40' E. It includes some of the most promising uranium occurrences which are related to the younger granite such as Um Had, Kab Amiri and El Erediya plutons. Also, it includes numerous old gold mines such as El Erediya, Atalla, El Fawakhir, El Sid and Hamama. There are numerous ancient gold diggings along a huge NW -SE shear zone which extends about 80km from El Erediya in the north to El Fawakhir in the south.*

The present work deals with the analysis and interpretation of airborne gamma-ray spectrometric and magnetic data of Bir Um Fawakhir area in order to explain the structural factors controlling the mineralization in this area. A set of radioelements (K%, eU_{ppm}, & eTh_{ppm}) contour maps as well as their ratio (eU/eTh, eU/K and eTh/K) maps were prepared. They are superimposed individually on the geological map to delineate uranium potentiality. The constructed maps revealed that the southern parts of both Kab Amiri and Um Had plutons as well as the northwestern part of El Erediya pluton are the most promising zones for uranium potentiality. The aeromagnetic data were analyzed and processed by several advanced techniques; reduction to the pole, regional-residual separation, second vertical derivative (SVD), analytical signal, Euler deconvolution and shadowgrams. Analysis of the structural lineaments of the Landsat image along with the geological map shows that most of the well-developed structural lineaments have NW - SE, NE-SW and N-S trends. The fault patterns as delineated from Landsat image are well matched with those obtained from analyzing aeromagnetic data. The mineralizations found along NW-SE fault zones appear as linear patterns. The basic magmatic activities that belong to the Red Sea rifting were intruded through these NW-SE deep-seated faults forming relatively long and narrow dykes as delineated from the aeromagnetic maps. The mineralizations of uranium and gold are controlled in their spatial distribution by fault tectonics and basic magmatic rock. Uranium and gold mineralizations are occurring along these NW-SE sub-parallel faults.

1- INTRODUCTION

Bir Um El Fawakhir area is confined between two paved roads namely, Qena-Safaga and Qift-Al Quisr roads that traverse the region in approximately ENE-WSW. Wadi Atalla is running in NW-SE and connect between both roads. Along this wadi many uranium and gold prospect areas were found including El Misskat and Elaridya U prospect and Atalla, Serbax, Abu Marawat, Hammama, and Fawakhir-El Sid gold deposits. The region is underlain by the Basement Complex of Precambrian rocks that are part of the

Nubian Shield. According to Essawy and Abu Zeid (1972), Atalla felsite is the longest felsite intrusion (19.5 Km long by 1 to 3 Km) was recorded in the basement complex of the eastern desert.

It was noted that, there is a certain linear pattern in the metallogenic map (Fig. 1) representing the spatial distribution of localities of both gold and uranium deposits in the study area. The linear arrangement of the uranium and gold deposits starts in the north from Fatira, Abu Marawat, Hamama, Gidami, Gebel Semna, Semna, Abu Grahish, Seg, Kab Amiri, Ereidiya, Atalla El Mur, Atalla, Rabshi, Um Esh, Um Had, El Fawakhir and El Sid in the south and extends to outside the study area through El Baramiya forming a NW-SE uranium-gold belt.

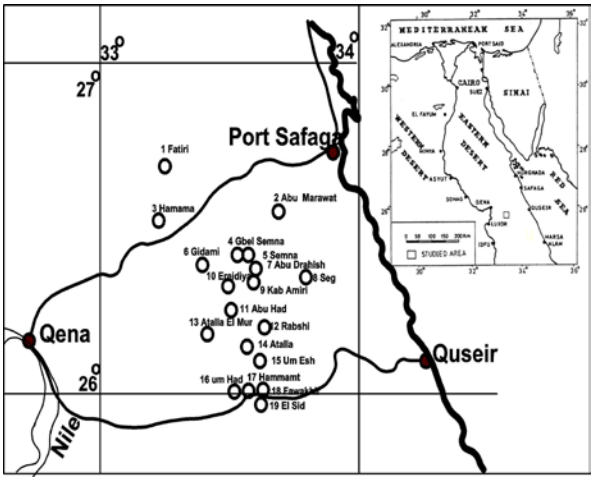

Fig. (1): Part of Metallogenic map of Egypt.

The main purpose of this work is to integrate the available airborne spectrometric and magnetic and satellite remote sensing data with the geological investigation in order to explain the structural factors controlling the mineralization in this area. This goal is achieved by manipulating various data sets separately and then integrating them together.

GEOLOGICAL SETTING

The regional geology of Bir Um El Fawakhir area is included in Geological Map of Quseir Quadrangle scale 1:250 (1992, EGSMA) and Conoco coral geological map of Quseir (NG36NE) scale 1:500,000 (CONOCO, 1987). It is also included in Akaad and Noweir (1969), El-Kassas (1974), Bakhit (1978), Akaad and Noweir (1980), El-Bouseily et. al., (1986) Bakhit and El-Kassas (1989), Abu El-Ela (1990), Fowler (2001) and Akawy (2007).

The regional geological setting is depicted in Fig. (2). It is comprised (starting with the oldest) of ophiolitic serpentinite, metagabbro, metavolcanics, metasediments, Hammamat clastics, younger granites, post-Hammamat felsite, Galala formation (Marine fossiliferous limestone intercalated by shale in the loser part) and Taref formation (fluviatile and locally eolian sandstones, fine-to-medium-grained with interbedded channel and soil deposits).

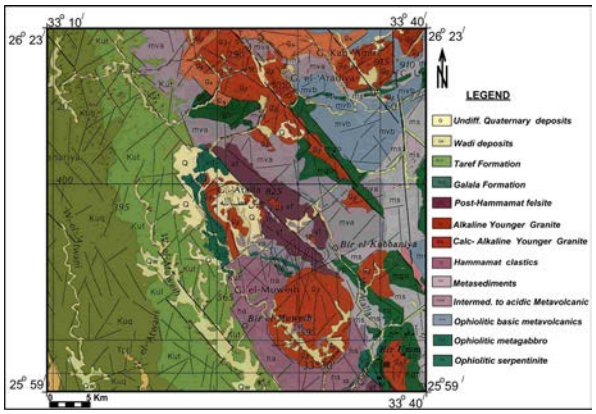

Fig. (2): geological map of Um El Fawakhir area, Central Eastern Desert, Egypt (Conoco Coral, 1987).

These rocks are dissected by numerous post granitic dykes of various compositions and traversed by several dry wadies, filled with Quaternary alluvium deposits. The exposed rock units could be arranged into five main groups from the older to the younger according to the recent studies, (El Gaby et. al., 1988 and Abdel Meguid, 1992).

- The Pre-Pan-African rocks (metasediments and gneisses, Greiling et. al., 1988).
- Pan-African ophiolites and island arc assemblage (metavolcanics, diorites and metagabbro).
- The island arc rocks (syntectonic to late tectonic diorite-granodiorite complex, gabbro and younger granite).
- Cretaceous sediments (Nubian and Post-Nubian sandstones) and alkaline volcanic rocks.
- Quaternary sediments (The more recent group).

MINERALIZATION

The study area includes many uranium and gold mining districts. The principal interest has been in gold. The world's most ancient mining map *"Wadi Hammamat*", region is located on Um El Fawakhir area. Wadi Hammamat region is shown on a papyrus map dating back to the times of Ramesses II.

Some significant radiometric anomalies in several younger granite plutons of the area was first detected by regional airborne radiometric and magnetic survey (Ammar, 1973). The existence of uranium mineralization was realized by surface and subsurface geologic, radiometric and mineralogical investigations (El-Kassas, 1974; Bakhit, 1978; El-Tahir, 1985; Bakhit et al, 1985; Abu-Deif, 1985 and1992; Hussein et al, 1986 and 1992; Hussein, 1987; Mohammed, 1988;

Abdel-Monem et al, 1990; Ahmed, 1991; Rabie and Ammar, 1990; Hussein and Sayyah, 1992; Abu-Deif et al, 1997; El-Sirafy, 1995; El-Kattan et al, 1995; Ibrahim, 2002; Amer et al, 2005; and Abu-Deif and El-Tahir 2007).

Uranium deposits are described as structurally controlled mineralization in El Erediya (El Kassas, 1974) and Kab Amiri areas (Bakhit, 1978). Uranium mineralization occurs in the marginal phase of the younger granite of El Erediya pluton (near the ancient El Erediya gold mine) in contact with metasedimentary rocks. The El Erediya uranium prospect contains several shear zones, some of which were locally mineralized on the surface. Similar relationships can be observed with the gold mineralization at the Gidami, Eleridiya and Atalla gold mines, where the auriferous quartz veins occur in hornblende-bearing igneous rocks of quartz-dioritic, granodioritic and grey granite composition close to their metasedimentary mantle rocks.

Gold Vein deposits are structurally controlled by the NE-SW and NW-SE trends (Mussa and Abu El Leil, 1983), occurring as vein type mineralization, being fissure fillings, confined to fault planes, or zones of intensive fracturing. The best occurrences in the study area for Gold occurrences are Abu Grahish, Kab Amiri, El Erediya, Abu Had, Rabshi, Atalla El Mur, Atalla, Um Esh, Um Had, Hammamat, El Fawakhir and El-Sid areas.

LANDSAT IMAGE

Landsat imagery was used as an aid to geological mapping and surface lineament delineation. Lithological units were identified from Landsat TM image (Fig. 3) along with the geological map based the analysis of the visual interpretation of colour composites. Based on tonal, textural difference, morphology and structure the separation of a crystalline basement complex has been inferred. The major lithological units identified are ophiolitic serpentinite, metagabbro, metavolcanics, metasediments, Hammamat clastics, younger granites, post-Hammamat felsite, Galala formation and Taref metavolcanics, Study of the Landsat image revealed that huge zone of Um Had pluton is covered by Hammamat clastics as roof pendant.

Visual analysis of Landsat image (Fig. 3) was utilized for identification of the lineaments and the surface structural features associated with mineralization. The basement complex is characterized by a great number of fracture lines of various trends. The statistical analysis of the extracted structural lineaments allowed constructing the rose diagrams presented in Fig. (4). Most of the well-developed lineaments (lengthwise or numberwise) have NW-SE, NE-SW and N-S. The NW-SE trend is common in all rock exposures in the study area and forming very long Wadis and lithological contact between basement and sedimentary rocks.

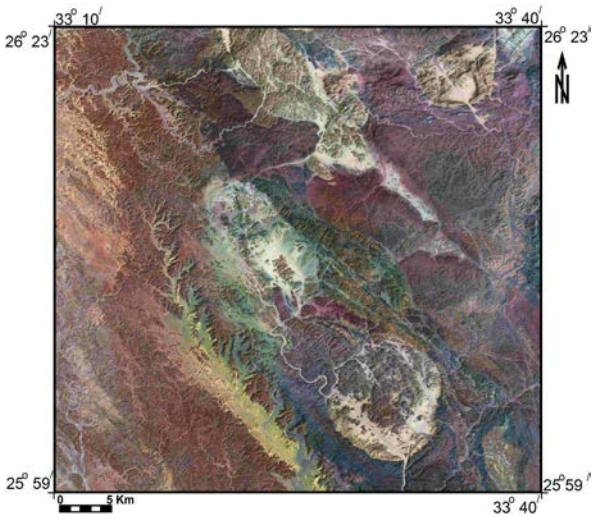

Fig. (3): False color composite Landsat image, Bir Um El Fawakhir area, Central Eastern Desert, Egypt.

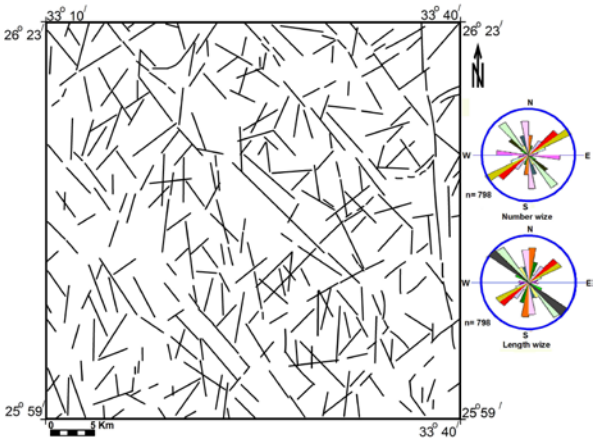

Fig. (4): The resultant frequency rose diagram of the interpreted surface structural lineaments, as deduced from the geological map and landsat image.

GEOPHYSICAL DATA

The airborne geophysical gamma-ray spectrometry and magnetic data were produced in 1984 by Aero service Division, Western Geophysical Company of America. The survey was conducted along parallel flight lines that were oriented in a NE-SW direction at one km spacing, while the tie lines were flown in a NW-SE direction at 10 km intervals.

A) Airborne Gamma-Ray Spectrometry (AGRS) Data Analysis:

Airborne gamma-ray survey provided important information about the distribution of K, U and Th in the area. Radioelements contour maps (K%, eUppm and eThppm) as well as ratio maps (eU/eTh, eU/K and eTh/K) were prepared. They are superimposed on the geological map of the area to determine the geochemical characteristics and evaluate the litho-structural features for the different rock exposures; this may help in the delineation of potential uranium targets, as well as for the purpose of identification and registration of the most important radioactive localities in this region.

Total Count (in Ur) Contour Map:

Total count map (Fig. 5) shows that, metavolcanics and metasediments have total-count level lower than 3 Ur. Generally, Galala formation is radioactively higher (4-6 Ur) than Taref formation (3-4 Ur). The younger granites delineated carefully by total-count level of 12 Ur and increases gradually towards the inner zones of the plutons reaching up to 18, 22 and 28 Ur at southeast Kab Amiri, southeast Um Had and northwest of El Erediya plutons respectively.

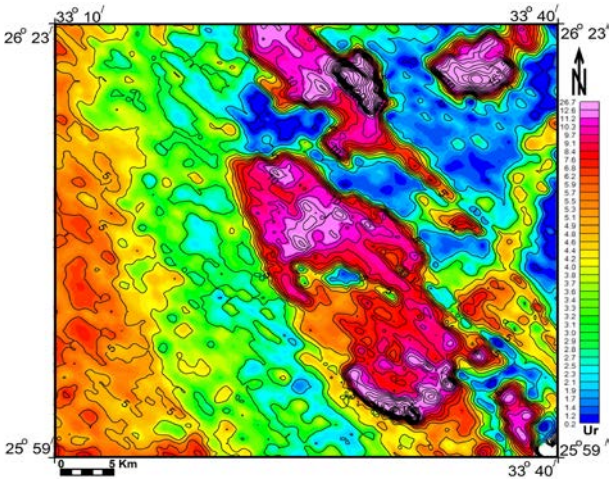

Fig. (5): Airborne total count contour map (in Ur), Bir Fawakhir area, Central Eastern Desert, Egypt.

Potassium Surface Distribution Contour Map:

Potassium is commonly found in potash feldspars, microcline, and orthoclase or in micas such as muscovite and biotite. Potassium map (Fig. 6) shows the over all spatial distribution of the relative potassium concentration. Metavolcanics and metasediments has potassium concentration lower than 0.5 K%.

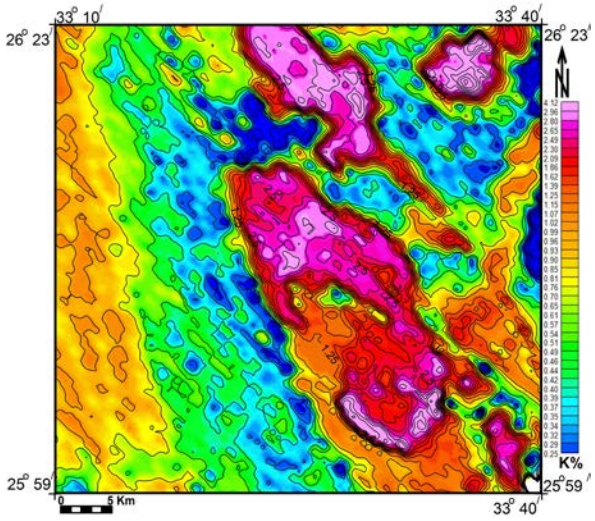

Fig. (6): Airborne potassium contour map (in %), Bir Um El Fawakhir area, Central Eastern Desert, Egypt.

Taref formation has potassium concentration up to 1 k% while; Younger granite plutons have K contents over 2.5 % reaching up to 3.5% at southeast Kab Amiri and Southeast Um Had. The general trend of K anomalies is NW-SE and NE-SW. It delineates areas where hydrothermal alterations associated with potassium enrichment might have occurred. This alteration zones are frequently associated with the formation of various types of non-radioactive mineral deposits e.g. Copper and gold deposits.

Uranium Surface Distribution Contour Map:

Uranium and thorium are usually found in accessory minerals such as apatite, sphene and zircon or in the rarer allanite, monazite, pyrochlore, thorite, uraninite, and xenotime. Both thorium and uranium content tend to be greater in felsic rocks and to also increase with alkalinity (Hoover et al., 1992).

Equivalent uranium map (Fig. 7) shows distinctive radioactive trends (NW-SE and NE-SW). The northwestern part of El Erediya and southeastern part of Um had plutons are the most promising zones for uranium potentiality. Younger granite plutons have eU contents over 5 ppm with the exception of the El Maghrabia pluton which has eU contents less than 4 ppm. The southeastern part of Um Had pluton has eU contents of 13 ppm. The northwestern part of El Erediya pluton has eU contents of up to 18 ppm.

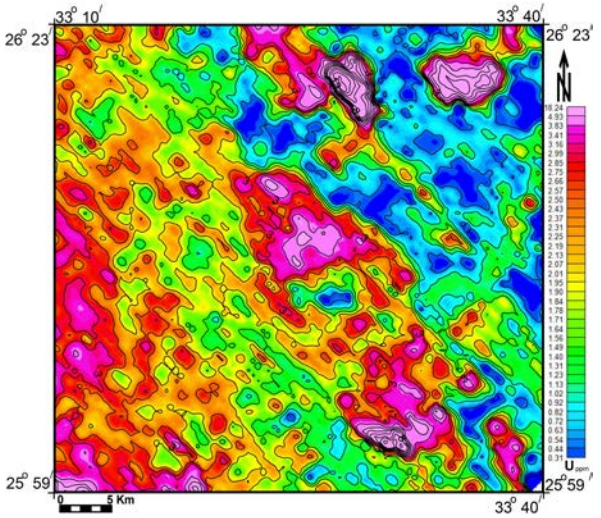

Fig. (7): Airborne equivalent uranium contour map (in ppm), Bir Um El Fawakhir area, Central Eastern Desert, Egypt.

Thorium Surface Distribution Contour Map:

Thorium is much less soluble than uranium and potassium and does not move except by mechanical means such as wind and erosion processes. Generally, thorium content is constant and when it increases this reflects fractionation in this type of granites. The thorium content contour map (Fig. 8) shows that the younger granites have eTh contents over 8 ppm. A noticeable fractionation toward the south was detected in the granitic pluton of Kab Amiri where the thorium content varies from 10 ppm at the north to 26 ppm at the

south. Meanwhile, at Um Had the thorium content varies from 10 ppm at the north to 28 ppm at the south due to the fact that, the northern part of Um Had pluton is covered by Hammamat clastics as roof pendants.

Generally thorium anomalies accompany the uranium ones. These anomalous zones are aligned along NW and NE trends.

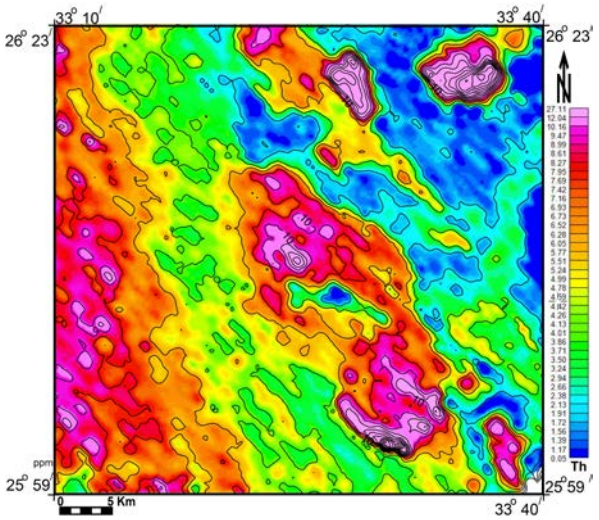

Fig. (8): Airborne equivalent thorium contour map (in ppm), Bir Um El Fawakhir area, Central Eastern Desert, Egypt.

Ratio maps (Th/K, U/Th, and U/k):

Bedrock concentrations are higher than airborne gamma-ray spectrometry values. Ratio patterns can enhance subtle variations in elemental concentrations due to lithological changes or alteration processes associated with mineralization meanwhile, ratio values (eU/eTh, eU/K and eTh/K) tend to closely approximate ratio values at ground level. Because of the strong correlation between the radioelements due to geochemical reasons, the maps of the radioelements are all very similar. Working with their ratios will therefore not only reduce disturbing effects, but also reduce the contrast of the image.

eTh/K ratio Contour Map:

The ratio between potassium and thorium is rather constant in most rocks, typically varying from 8.5 to 10 ($Th_{ppm}/K_{\%}$, Hoover et al, 1992). Rocks with Th /K ratios significantly outside this usual range have been called potassium or thorium specialized (Portnov, 1987).

Igneous rocks with potassium specialization have been related to gold-silver, silver-polymetallic, molybdenum, and bismuth deposits. Thorium specialized rocks are identified with tin, tungsten, rare-earth, and rare-metal deposits (Portnov, 1987). Accordingly, south of both Um Had and Kab Amiri plutons (Fig. 9) are considered as thorium specialized rocks.

eU/eTh ratio Contour Map:

In general, the granitic areas has high eU/eTh ratio compared to the normal crustal ratio of 0.28 (Clarke, et al., 1966) are described as uranium enrichment areas. eU/eTh reaches up to one (Fig. 10) in the episynite zone at southern Kab Amiri pluton. It is very promising target.

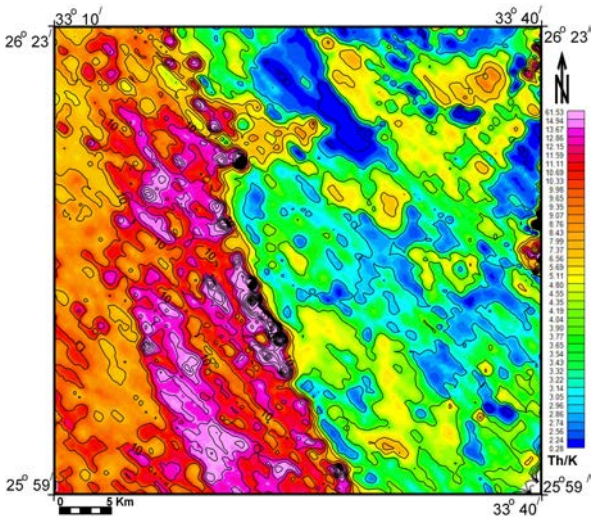

Fig. (9): Airborne eTh/K ratio contour Bir Um El Fawakhir area, Central Eastern Desert, Egypt.

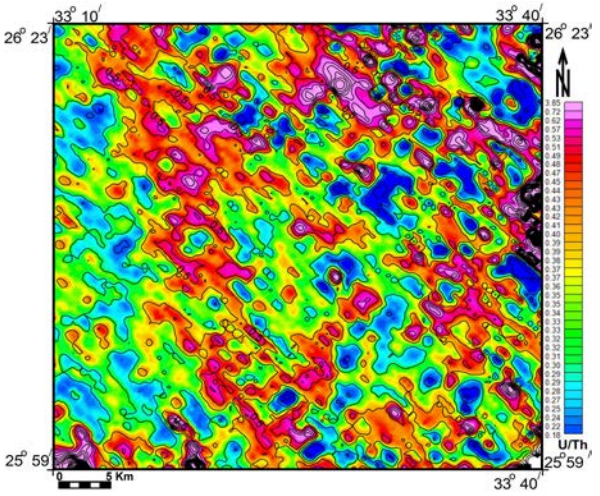

Fig. (10): Airborne eU/ eTh ratio contour, contour Bir Um El Fawakhir area, Central Eastern Desert, Egypt.

eU/K ratio Contour Map:

The younger granites have eU/K ratio more than 2 (Fig. 11). El Maghrabia pluton has eU/K ratio less than 2. Northern western part of El Erediya pluton has eU/K ratio up to 6.

Ternary Radioelement Map:

This map (Fig. 12) is a three-element display of equivalent uranium (ppm), equivalent thorium (ppm), and potassium (%). Uranium is displayed in red hues, thorium in green, and potassium in blue. Different ratios of the three elements are displayed as RGB color combinations. Regions with relatively high

concentrations of all elements look white; regions with relatively low concentrations of all elements look dark gray. Each color band is nonlinear quantized using a histogram stretch to ensure a relatively uniform distribution of levels and to enhance low-contrast areas.

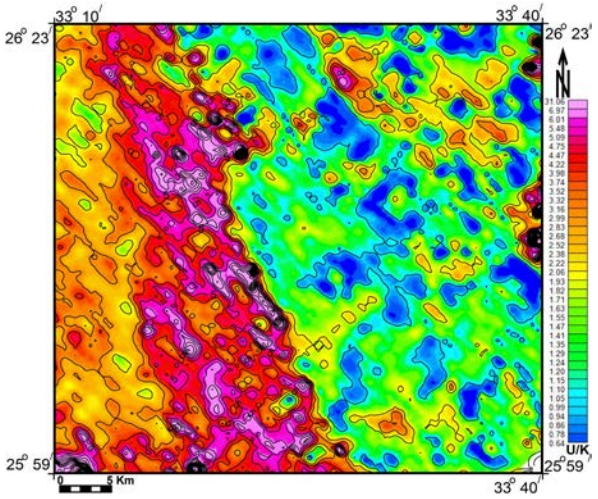

Fig. (11): Airborne eU/K ratio contour, contour Bir Um El Fawakhir area, Central Eastern Desert, Egypt.

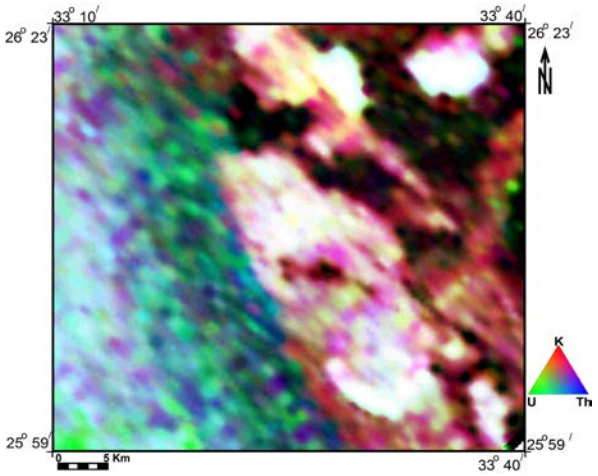

Fig. (12): Ternary radioelement map, Bir Um El Fawakhir area, Central Eastern Desert, Egypt.

In many cases, particular rock types will have characteristic ratios of the three elements and this type of map display can highlight useful geologic trends and patterns. In addition to distinguishing lithologic variations, because of the contrasting chemical properties of the radioactive elements, radiometric data can provide information relevant to understanding of various geochemical and physical processes, including alteration and weathering (Duval, 1989). Bright spots are areas where K is higher than predicted and may be areas of K-alteration, an indicator of mineralized areas.

b) Analysis and interpretation of Aeromagnetic Data:

Processing of the available aeromagnetic data was carried out using Geosoft mapping and processing system (Geosoft, 1999). The total magnetic intensity field data (Fig. 13). were transformed to the wave-number domain. Reduction to the north magnetic pole was performed at the first stage of processing of aeromagnetic data (Fig. 14). It reduces the anomalies to those that would be observed at the magnetic north pole with a vertical remnant magnetization direction.

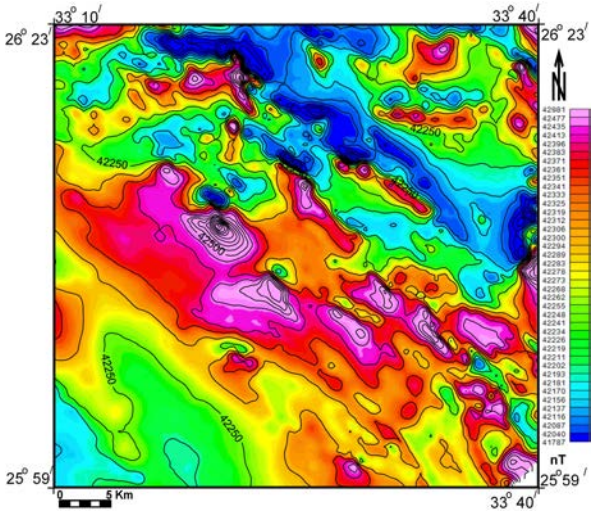

Fig. (13): Total aeromagnetic intensity map, Bir Um El Fawakhir area, Central Eastern Desert, Egypt.

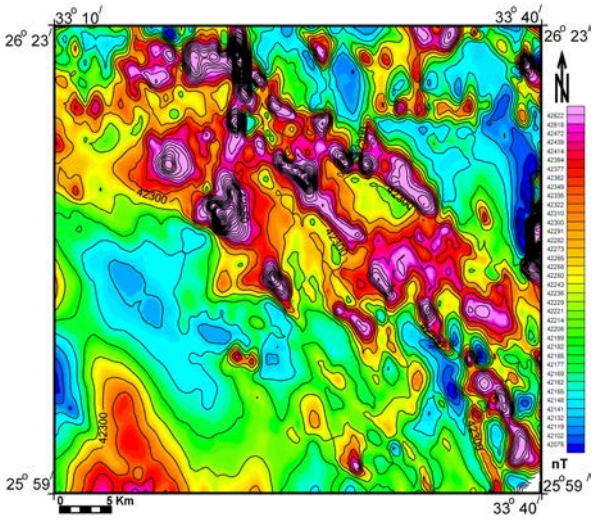

Fig. (14):Reduced to pole (RTP) aeromagnetic map, Bir Um El Fawakhir area, Central Eastern Desert, Egypt.

The second step is to separate the total field using the band-pass filter conducted for the RTP into deep regional and shallow residual components. Therefore, the azimuthally averaged logarithmic power spectra were computed (Fig. 15).

The log spectrum shows two segments representing the regional and residual components, where spectral slope technique was applied to each. The residual map (Fig. 16) exhibits the local anomalies which reflect the near-surface structures at about 500m depth, while the regional map (Fig. 17) reflects the broad anomalies related to the regional changes in the structures of the basement rocks. The most interesting

phenomenon is the occurrence of subparallel faults system of linear aeromagnetic anomalies running NW-SE parallel to Red Sea and Gulf of Suez trend. The second vertical derivative technique (Fig. 18) was applied on the regional component. SVD map for the regional component of RTP succeeded to delineate the contacts between lithologies with contrasting magnetizations. It has negative (downthrown) parts and positive (upthrown) parts. The zero line succeeded also to delineate carefully faulted structures.

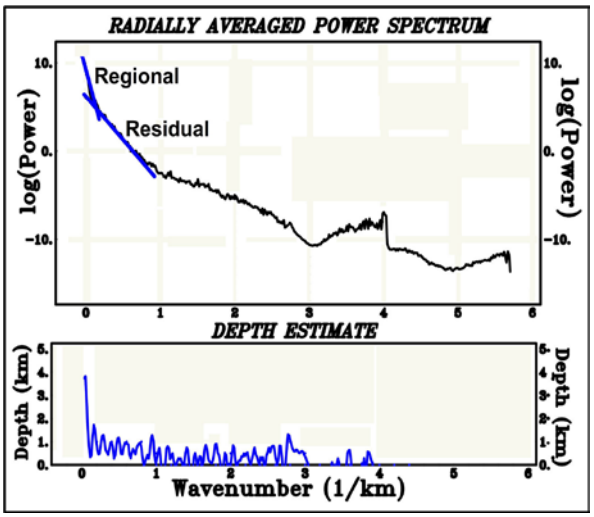

Fig. (15): A typical energy power spectrum curve of the RTP data.

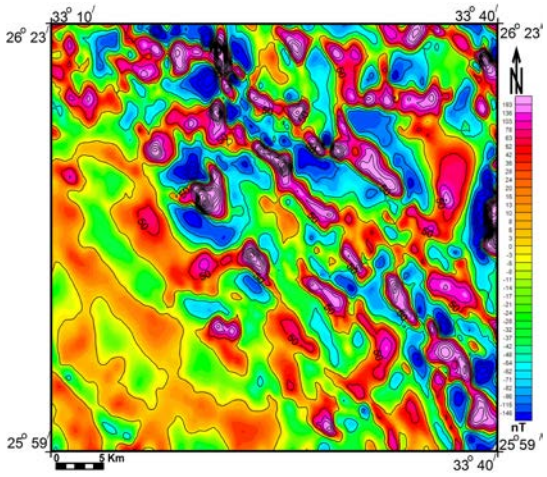

Fig. (16): Residual component of RTP map, Bir Um El Fawakhir area, Central Eastern Desert, Egypt.

Another useful interpretational tool is the analytical signal (Nabighian, 1972, 1984) was carried out (Fig 19). It reveals the presence of a linear aeromagnetic anomalies running through sub parallel NW-SE regional faults for many kilometers along the contacts of metasediments, metavolcanics, Hammamt sediments and granites. These NW faults are injected with basic dykes.

Generation of shadowgram for the regional magnetic map (Fig. 20) reveals several shear zones are favorable zones for gold deposits. This procedure treats a potential-field map as a relief, and computes the shadow pattern that would be created if this relief was illuminated by the sun from a user-specified angle. Subtle, local and short-wavelength anomalies are emphasized. Side-lighting (non-vertical illumination) acts as a directional filter. Side-lighting enhances anomalies non-parallel to the "sun" azimuth, and many shadowgrams with various sun angles were needed to reveal variously oriented anomalies.

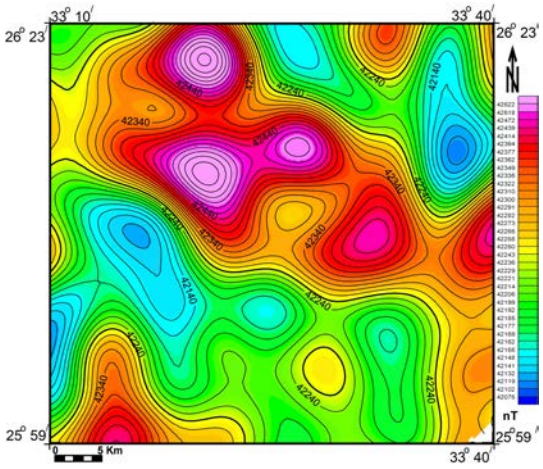

Fig. (17): Regional component of RTP map, Bir Um El Fawakhir area, Central Eastern Desert, Egypt.

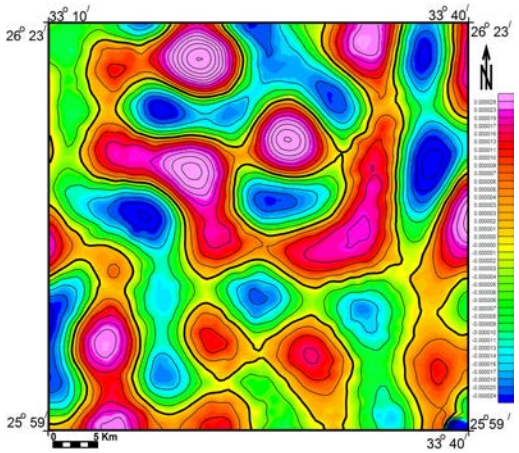

Fig. (18): SVD of Regional component of RTP map, Um El Fawakhir area, Central Eastern Desert, Egypt.

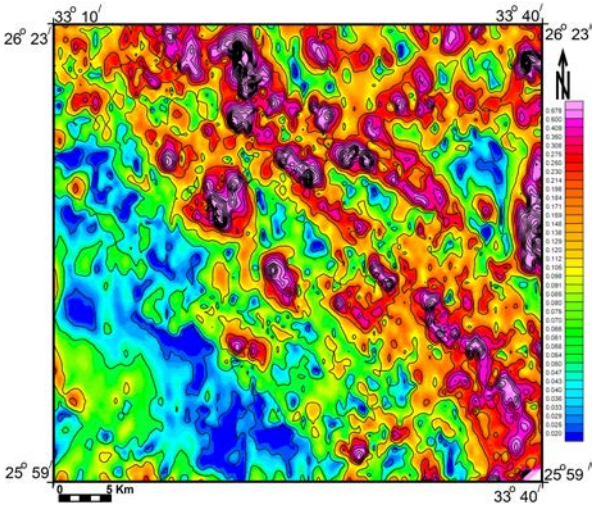

Fig. (19): Analytic Signal map, Bir Umm Fawakhir area, Central Eastern Desert, Egypt.

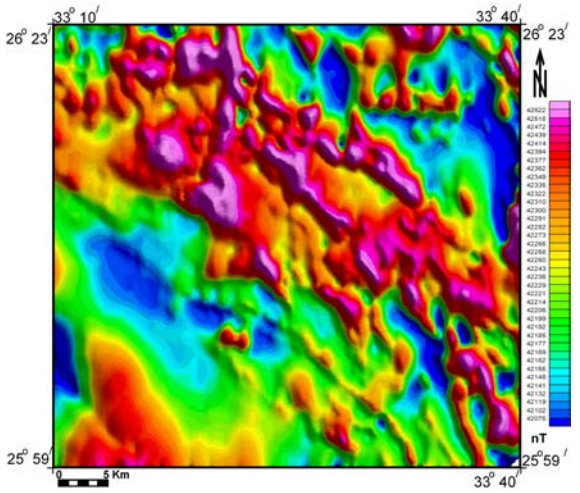

Fig. (20): Shadowgrams of Regional component of RTP map, Bir Umm Fawakhir area, Central Eastern Desert, Egypt.

Euler deconvolution method is a profile-based or map-based depth estimation method based on the concept that the magnetic fields of localized structures are homogeneous functions of the source coordinates and therefore satisfy Euler's equation (Reid et al., 1990).

$$(x-x_0)\partial\Delta T/\partial x+(y-y_0)\partial\Delta T/\partial y+(z-z_0)\partial\Delta T/\partial z=-S_i\Delta T$$

Where, (x,y,z) is the position at which the total field anomaly is ΔT, arising from a source at position (x_0,y_0,z_0). S_i is the 'structure index' (SI) of the source geometry (Thompson, 1982). An SI of 3 corresponds to a point source (dipole), 2 is appropriate for extended line sources, such as pipes and cylinders, a value of 1 for a step, thin dike or sill edge, and values of 0.5 and 0 have been chosen for faults and other contacts (Reid et al., 1990).

Figures (21) show the Euler solution of contacts (SI=0) with different symbols proportional to depth at the source positions. It clearly pronounces the NW-SW and NE-SW direction as predominant structural trends controlling the structural framework of the area. The symbols and clusters align themselves in a linear pattern on this trend for the selected structural index of contacts.

The results of the previous analyses were integrated with the surface and subsurface geological information to construct the interpreted basement tectonic map (Fig. 22). This map reveals that, the main structures recognized in this area are a set of NW-SE fault system intersected by a set of NE-SW faults. Most of the mineral deposits have the same trends as faults and basic dykes and in many areas superimposed with them. The common favorable condition for gold and U mineralizations is the decrease of their mobility, which is achieved by relative increase of CO2 that act as reducing agents due to the injection of basic magma. This may give a clue explanation of accompany their.

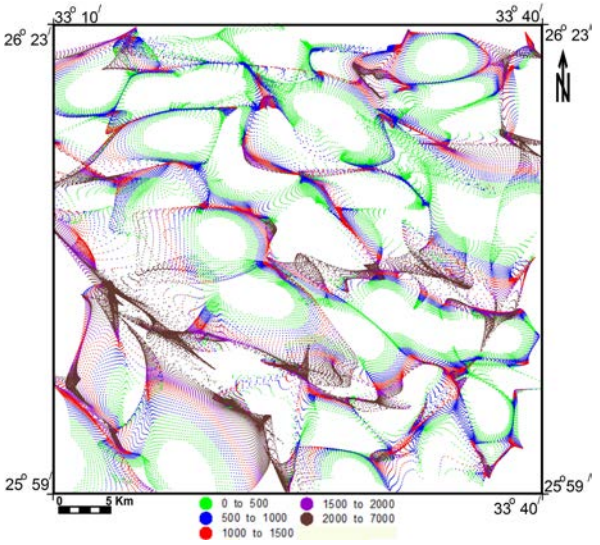

Fig. (21): Euler solution of contacts, , Bir Umm Fawakhir area, Central Eastern Desert, Egypt.

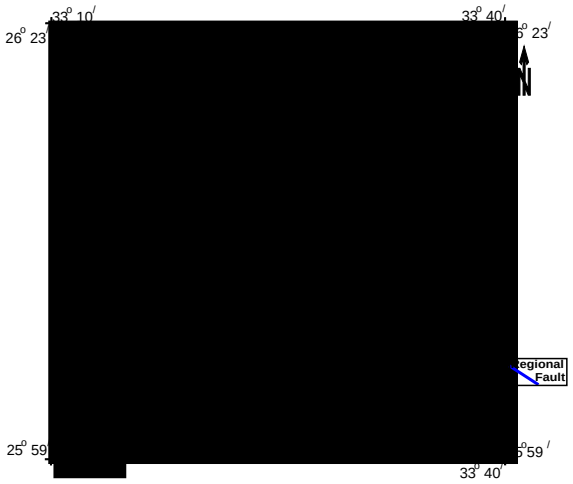

Fig. (22): Basement tectonic map of the area, Bir Umm Fawakhir area, Central Eastern Desert, Egypt.

SUMMARY AND CONCLUSION

It was noted that the locations of the well known uranium and gold occurrences in the study area have distinctive linear pattern. The main purpose of this work is to integrate the available airborne geophysical data and satellite remote sensing data with the field geological investigation in order to explain the structural factors controlling mineralization in this area.

The airborne gamma-ray spectrometric and aeromagnetic data were analyzed and interpreted to achieve these goals. The analysis and interpretation of geophysical data reveal that, these well known uranium and gold mineralization occurrences, aligned along NW-SE sub-parallel shear zones, are crosscut by NE-SW regional fault system. Landsat imagery was used as an aid to geological mapping and surface lineament

delineation. Landsat image revealed that the northern part of Um Had pluton is covered mainly by Hammamat clastics as roof pendants. Most of the well-developed lineaments (in lengthwise or numberwise) have NW-SE, NE-SW and N-S trends.

Radioelements (K%, eU_{ppm}, & eTh_{ppm}) contour maps and their ratio (eU/eTh, eU/K and eTh/K) maps helped in delineation of potential uranium targets. The most promising zones for uranium potentiality are the southern parts of the main pluton of Kab Amiri, the episynite zone to the south of Kab Amiri pluton and southern part of Um Had pluton as well as the northwestern part of El Erediya pluton.

The faults pattern (NW-SE, NE-SW and N-S) in the area is well matched with the magnetic lineaments and the radioelements anomalies which suggest the role of basic magmatic activity along the NW-SE trend in controlling the mineralization.

REFERENCES

Abdel Meguid, A. A., 1992: Late Proterozoic Pan African tectonic evolution of the Egyptian part of the Arabian-Nubian Shield. M. E. R. C. Ain Shams Univ., Earth Sc. Ser., Vol. 6, pp 13-28

Abdel-Monem, A, A., Bakhit, F. S., and Ali, M. M, 1990: Trace and rare earth elements geochemistry of the uranium mineralization at El-Erediya, Central Eastern Desert, Egypt, Egyptian Mineralogists, 2.143-150**.**

Abu El-Ela, F.F., 1990: Supra-subduction zone ophiolite of Qift-Quseir Road, Eastern Desert, Egypt. Bulletin Faculty Science Assiut University, Egypt 19, 51-70.

Abu-Deif A.; 1985: Geology of uranium mineralization in El-Missikat area, Qena-Safaga road, Eastern Desert, Egypt. M. Sc. Thesis, Al-Azhar Univ., Cairo, 103 p.

Abu-Deif A., 1992: The relation between the uranium mineralization and tectonics in some Pan-African granites, west of Safaga, Eastern desert, Egypt. Ph. D. Thesis, Assiut Univ., Egypt, 218 p.

Abu-Deif A., Ammar, S. E. and Mohamed, N. A.; 1997: Geological and geochemical studies of black silica at El-Missikat pluton, Central Eastern Desert, Egypt. Proc. Egypt. Acad. Sci. 47, pp. 335-346.

Abu-Deif A., El-Tahir, M. A., 2007: A new uranium occurrence, Gabal El-Missikat prospect, Central Eastern Desert, Egypt. Jour. of king Abdulaziz Univ., earth Sciences.

Aeroservice, 1984: Final operational report of airborne magnetic-radiation survey in the Eastern Desert, Egypt, for the Egyptian General petroleum Corporation. Aero Service, Houston, Texas, April, 1984, six Volumes.

Ahmed, N. A; 1991: Comparative studies of the accessory heavy minerals in some radioactive rocks of G. El-Misskat and G. El-Erediya, Eastern Desert, Egypt and their alluvial deposits, M. Sc. Thesis, Cairo Univ., Egypt, 244p.

Akaad, M.K. and Noweir, A.M., 1969: Lithostratigraphy of the Hammamat Um Seleimat district, Eastern Desert, Egypt. Nature, v. 223, pp. 284-285.

Akaad, M.K., Noweir, A.M., 1980: Geology and lithostratigraphy of the Arabian Desert erogenic belt of Egypt between Lat. 25O35' and 26O30'. Institute Applied Geology, Jeddah, Bulletin 4, 127-l 34.

Akawy, A. 2007: Geometry and texture of quartz veins in Wadi Atalla area. Central Eastern Desert, Egypt. Journal of African Earth Sciencs. Volme 47. Issue 2. February 2007. Pages 73-87.

Amer, T. E.; Ibrahim, T. M. and Omer, S. A; 2005: Micro-prope studies and some rare metals recovery from El- Missikat mineralized shear zone, Eastern Desert, Egypt. The Fourth International Conferrence of the Geology of Africa, Nov. 2005, Assiut, Vol.(2), p-p 225-238.

Ammar, A. A. 1973: Application of aerial radiometry to the study of the geology of Wadi El-Gidami, Eastern Desert, Egypt. (with aeromagnetic application). Ph. D. Thesis, Faculty of Science, Cairo University, Geiza, Egypt. 424 p.

Bakhit, F. S.; 1978: Geology and radioactive mineralization of El-Missikat area, Eastern Desert, Egypt. Ph. D. Thesis, Ein Shams Univ., Cairo, Egypt, 289 P.

Bakhit, F. S., P. D., Assaf, H. A. and Abu Dief, A., 1985: Correlation study on the geology and radioactivity of surface and subsurface working at El-Misskat area, Central Eastern Desert, Egypt. Mining Geology. Contr. mineral geology, 35(5), 345-354p.

Bakhit F. S. and El-Kassas I. A., 1989: Geology of wadi Atalla-El Missikat area, Eastern Desert, Egypt. Qatar Univ. Sci. Bull. Vol. (9), P227-244.

Broome, J., Carson, J.M., Grant, J.A., Ford, K.L., 1987: A modified ternary radioelement mapping technique and its application to the south coast of Newfoundland: Geological Survey of Canada Paper 87-14, 1 sheet, scale 1:500,000.

Clark, S. P., Jr., Peterman, Z. E. and Heier, K. S., 1966: Abundance of uranium, thorium and potassium. *Handbook of Physical Constants*. Geol. Soc. America, Mem., no. 97, p. 521-541.

CONOCO, 1987: Geological map of Egypt (1:500,000 in 20 sheets): Conoco Coral and Egyptian General Petroleum Corporation (Cairo).

Duval, J.S., 1989 : Radioactivity and some of its applications in geology, in "Proceedings of the Symposium on the Application of geophysics to Engineering and Environmental Problems", SAGEEP 89, March 13-16, Golden, Colorado, p. 1-61.

El Gaby, S., Franz, K. and Resa Tehrani, 1988: Geology, evolution and metallogenesis of the Pan-African belt in Egypt. In E' Gaby and R. 0. Grielling (eds.). The Pan-African belt o Northeast Africa and adjacent area. Earth Evol. Sci., 1988 Andreas. Vogel, Berlin.

El Kassas., I.A., 1974: Radioactivity and geology of Wadi Atalla area. Eastern Desert of Egypt, A.R-E. Ph.D. Thesis. Ain Shams Univ., Cairo, 502p.

El Kattan, E.M., Sadek, H.S., H.S., Rabie, S.I., Hassanein, H.I. 1995: Ground geophysical study for development and exploration of El-Misskat radioactive mineral prospect, Central Eastern Desert of Egypt. Nuclear geophysics, vol. 9, no. 4, p 3363-382.

El Sirafy, A. M., 1995: Generation and interpretation of the false colour composite images of the remotely-sensed multi-source geophysical data a sample area from the central Eastern Desert of Egypt. M.E.R.C. Ain Shams Univ., Earth Sci., Vol. 9, p.42-60.

El-Bouseily, A.M., Arslan, A.I., Ghoneim, M.F., Harraz, HZ., 1986: Mercury dispersion patterns around El Sid – Fawakhir Gold Mine, Eastern Desert, Egypt. Journal African Earth Sciences 5, 465-469.

El-Tahir, M. A. 1985: Radioactivity and mineralization of granitic rocks of El-Erediya occurrence and comparison to El-Misskat-Rie-El-Garra occurrence, Eastern Desert, Egypt; Ph.D. Thesis, Al-Azhar Univ., Cairo, 132p.

Essawy, M. A.,and Abu Zeid, K. M., 1972: Atalla felsite intrusion and its neighboring rhyolitic flows and tuffs, Eastern Desert. Annal of the Geo. Sur. of Egypt Vol.2, p. 270-280.

Fowler T.J., 2001: Pan-African granite emplacement mechanisms in the Eastern Desert, Egypt. Journal of African Earth Sciences, Vol. 32, NO. 1, pp. 61-66.

Geological Survey of Egypt, 1992: Geologic map of Al Qusayr Quadrangle, Egypt. Scale 1.250.000. Cairo, Egypt.

Geosoft Inc., 1999: GM-SYS modelling of potential field data. Geosoft Inc., Toronto, Canada.

Greiling, P.O., Kroner, A., El Ramly, M.F. and Rashwan, A.A., 1988: Structural relationships between the southern and central part, of the Eastern Desert of Egypt: Details of a fold and thrust belt. In: S. El Gaby and R.O. Greiling (Editors), The Pan-African of NE Africa and Adjacent Areas, Vieweg, Wiesbaden, PP. 121-145.

Hoover, D.B., Heran, W.D., and Hill, P.L., 1992: The geophysical expression of selected mineral deposit models: U.S. Geological Survey Open-File report 92-557, 129 p.

Hussein, H. A. H., 1987: Geochemistry of granitic rocks and uranium mineralization in El-Missikat-El-Erediya area, SW Safaga, Eastern Desert, Egypt, Ph.D. Thesis, Cairo Univ., Egypt, 254p.

Hussein, H. A., Hassan, M. A., EL-Tahir, M. A, and Abu-Deif, A., 1986: Uranium bearing siliceous veins in younger granites, Eastern Desert, Egypt, Report of the Working Group on Uranium Geology, I. A. E. A., Vienna, TECDOC, 361, 143-157.

Hussein, H. A. and Sayyah T. A. 1992: Uranium potential of Younger granites of Egypt, IAEA, Viena, Austria, 26-29p.

Hussein, H. A., EL-Tahir, M. A., and Abu-Deif, A., 1992: Uranium exploration through exploratory mining work, South Qena-Safaga midway, Eastern Desert, Egypt, 3rd. Mining, Petroleum and Metallurgy Conference, Cairo Univ., 1, 92-105.

Ibrahim, T. M.; 2002: Geologic and radioactive studies of the basement-sediment contact in the area west Gabal El-Missikat, Eastern Desert, Egypt. Ph. D. Thesis, Faculty of Science, Mansoura University, Mansoura, Egypt.

Mohammed, N. A.; 1988: Mineralogical and petrographical characteristics of some alteration products related to U-mineralization in El-Missikat- El Erediya areas, Eastern Desert, Egypt. M. Sc. Thesis, Cairo Univ., 110 P.

Mussa M.A. and Abu El Leil I., 1983 : Structural analysis as a guide to mineralization trends in the north eastern desert of Egypt. Annal of the Geol. Sur. Egypt, V. XIII. PP. 271-276.

Nabighian, M. N., 1972: The analytic signal of two-dimensional magnetic bodies with polygonal cross-section: Its properties and use for automated interpretation": Geophysics, 37, 507–517.

Nabighian, M. N., 1984: Toward a three-dimensional automatic interpretation of potential field data via generalized Hilbert transforms: Fundamental relations: Geophysics, 49, 780–786.

Portnov, A.M., 1987: Specialization of rocks toward potassium and thorium in relation to mineralization: International Geology Review, v. 29, p. 326-344.

Rabie, S.I., and Ammar, A.A.; 1990: Delineation of geological structures from aeromagnetic data using some integrated interpretation techniques, El

Misskat-El Erediya plutons, Centeral Eastern Desert, Egypt. The 8Th Annual Meeting of the Egyptian Geophysical Society (G.P.C), cairo, Egypt, pp. 111-134.

Reid, A. B., Allsop, J. M., Granser, H., Millett, A. J., Somerton, I. W., 1990: Magnetic interpretation in three dimensions using Euler deconvolution. Geophysics Vol. 55, PP. 80-91.

Space Atlas of Misr, 1990 Scale 1:25000: Remote Sensing Center, Acad. of Sc. Res. and Tech., Cairo, Egypt. Vol. 2.

The Mineral Map of Egypt, 1994: Egyptian geological survey and mining authority the mineral map of Egypt (explanatory notes and lists).

Thompson, D. T., 1982: EULDPH- A technique for making computer-assisted depth estimates for magnetic data. Geophysics Vol. 47, PP. 31-37.